On the Consequences of Microstructural Evolution on Macroscopic Behavior for Unsaturated Soils

Hiram Arroyo[1(✉)], Eduardo Rojas[2], Jatziri Y. Moreno-Martínez[1], and Arturo Galván[1]

[1] Universidad de Guanajuato, Celaya, Mexico
hiramarroyo@gmail.com
[2] Universidad Autónoma de Querétaro, Querétaro, Mexico

Abstract. Volumetric behavior of soils is amongst the most important parameters to be taken into consideration to describe many aspects regarding the hydro-mechanical coupling of unsaturated soils, such as the behavior of CO2 reservoirs subjected to moisture gradients, or the initiation of cracks due to suction loading-reloading.

Experimental observations show a clear transition of compressibilities as soils reach unsaturated states when tested under suction increments. This is termed shrinking limit. We address this behavior taking into consideration the evolution of pores where a mechanism of pore deformation is proposed to predict this shrinking limit. This model requires no other parameter than the initial pore-size distribution of the material.

1 Introduction

It is believed that the explanation for every observation regarding the mechanical behavior of soils lies on clarifying the mechanism of how pores behave on the presence of the liquids that they appertain within their pores.

When it comes to volumetric strains, experimental observations indicate that the compressibility due to suction increments highly decrease on the transition to saturated states. This transition has been identified by Perón (2008) as the shrinking limit where different compressibilities are needed to describe macroscopic evolution of volume strains. Constitutive models take this into consideration adding parameters to identify this transition, however, this increases the number of needed tests to calibrate such models.

Authors believe that conceptualizing the evolution of the pore-size distribution is the key to understand and predict macroscopic evidences such as the shrinking limit. Experimental observations evidence that pore-size distribution of soils exhibit most of the times a bimodal distribution (Alonso et al. 2010; Cui et al. 2002; Koliji et al. 2006). This pore-size distribution is related to macroscopic observations, as has been reported that macro-pores are the ones responsible for most of volume change observed. There is on the other hand a micro-pore distribution that suffers negligible changes as suction is applied. Here, suction influence on volumetric behavior is predominant when the soil is in a saturated state (Perón et al. 2009).

L. Hoyos and H. Shehata (Eds.): GeoMEast 2019, SUCI, pp. 56–66, 2020.
https://doi.org/10.1007/978-3-030-34206-7_5

This paper aims at proposing a mechanism for pore-size distribution evolution with suction increments to predict the shrinking limit of materials and the evolution of water retention properties of soils.

2 The Squared Grid Model

Because the internal structure of soils is too complicated to be modeled, the pore structure is simplified to regular geometries. It has been shown that the porous network contained within solid particles, can be modeled considering two main types of entities: sites and bonds. Sites contribute with most of the void space available for deformation and are responsible for every macroscopical aspect of soils that involves volumetric strains. Bonds interconnect sites and have little contribution to the volume of voids (Fig. 1).

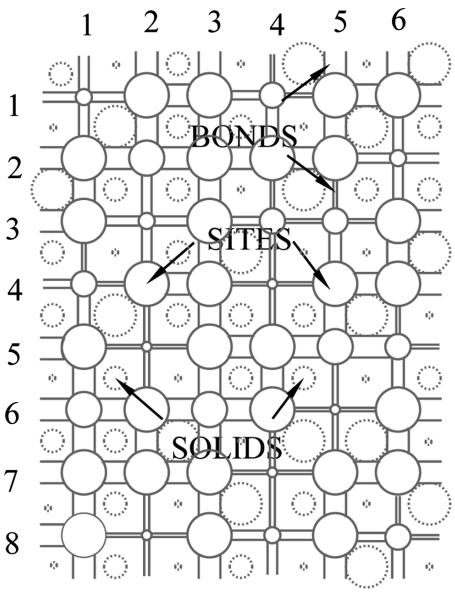

Fig. 1. Porous network used to model the porous space of soils (Arroyo and Rojas 2019).

The grid is composed of a set of interconnected sites. The connection elements between sites are called bonds. One solid particle is contained within a set of four sites interconnected by four bonds.

3 The Solid-Porous Model by Rojas

3.1 Modelling Pore-Size and Grain-Size Distributions

A first approach is to consider that all soil particles appertain a regular circular shape for the case of a 2D problem (spherical when it comes to dealing with 3D situations).

In order to make the model as real as possible, the frequency $f = n/N$ needs to be established. The frequency f with which each class of grains (i.e. set of n solid grains having the same size) appears within a soil sample, is referred to its total number of grains N. Here, to model f, a normal logarithmic density function is used:

$$f(R) = \frac{1}{\sigma R\sqrt{2\pi}} \exp\left[\frac{-(\ln R - \mu)^2}{2\sigma^2}\right] \tag{1}$$

Where, $f(R)$ is the frequency distribution of the class of grains of size R contained within the soil sample. Considering the network of solid grains, the volume of grains of size R is given by:

$$V^{SOL}(R) = N\pi \int_R^{R+dR} f(R)R^2 dR \tag{2}$$

Moreover, because soils can appertain clayey size particles, as well as sand particles, two functions can be used. Therefore, Eq. (2) can be expressed as $V^{SOL}(R) = N\pi \int_R^{R+dR} (f^{MSOL}(R)R^2 + f^{mSOL}(R)R^2)dR$. An additional degree of freedom is provided to model the GSD. This is, the inclusion of factor F^p_{SOL}, which is necessary to include due to the logarithmic scales of Eq. (1). This factor reduces the height of f^{MSOL}. Therefore, Eq. (2) can be expressed as:

$$V^{SOL}(R) = N\pi \int_R^{R+dR} \left(F^p_{SOL} f^{MSOL}(R)R^2 + f^{mSOL}(R)R^2\right)dR \tag{3}$$

The process to model the Pore-Size Distribution (PSD) is analogous to the one followed for the GSD. The following equation is used for the PSD:

$$V^S(R) = N\pi \int_R^{R+dR} \left(F^p_S f^{MS}(R)R^2 + f^{mS}(R)R^2\right)dR \tag{4}$$

Functions f^{MS} and f^{mS} are used to model the PSD of materials that appertain two classes of pores (large and small). Because soils are highly heterogeneous materials, the individual solids they contain have very different ranges of sizes. This double structure is produced by the compaction process and the initial way in which the soil sample was set up in the testing device. To differentiate two classes of sites, the terms "macro-sites" and "micro-sites" will be used regardless other classifications.

Contrary to the case of f^{MSOL} and f^{mSOL}, parameters controlling PSD functions are not constant. This implies that solid phase is incompressible, the void phase is not. The behavior of these two functions is the key of this work and it is believed that every single aspect of volumetric behavior (saturated and unsaturated), and the way to conceal saturated and unsaturated soil mechanics at the highest level using a simple constitutive model, such as the Cam Clay (Roscoe and Burland 1968), can be done by correctly modeling their behavior.

A pore-size distribution for bonds is also required, since the size of the interconnections between site elements depend on the size of the pores they interconnect.

$$V^B(R) = N\pi \int_R^{R+dR} \left(F_B^p f^{MB}(R)R + f^{mB}(R)R\right)dR \tag{5}$$

3.2 GSD and PSD Models to Determine the Void Ratio of the Material

Integrating both, Eqs. (3) and (4), over the whole range of possible sizes of particles allow determining the total volume of solid phase $\overline{V^{SOL}}$ and void phase $\overline{V^S}$. Therefore, void ratio can be expressed as:

$$e = \frac{\overline{V^S}}{\overline{V^{SOL}}} = \frac{N_S\pi \int_0^{\inf} \left(F_S^p f^{MS}(R)R^2 + f^{mS}(R)R^2\right)dR}{N_{SOL}\pi \int_0^{\inf} \left(F_{SOL}^p f^{MSOL}(R)R^2 + f^{mSOL}(R)R^2\right)dR} = \frac{N_S\overline{V^S}^*}{N_{SOL}\overline{V^{SOL}}^*} \tag{6}$$

3.3 Determination of Parameters for the GSD and PSD

Parameters to evaluate Eq. (3) describing material GSD are μ_{SOL}^M, σ_{SOL}^M, μ_{SOL}^m and σ_{SOL}^m. This is, a set of μ and σ parameters for both f^{MSOL} and f^{mSOL}. These are determined by a fitting procedure where the goal is to graphically superimpose the differential GSD of the material. The real GSD is obtained by any experimental means. Figure 2 is an example of the usage of Eq. (3).

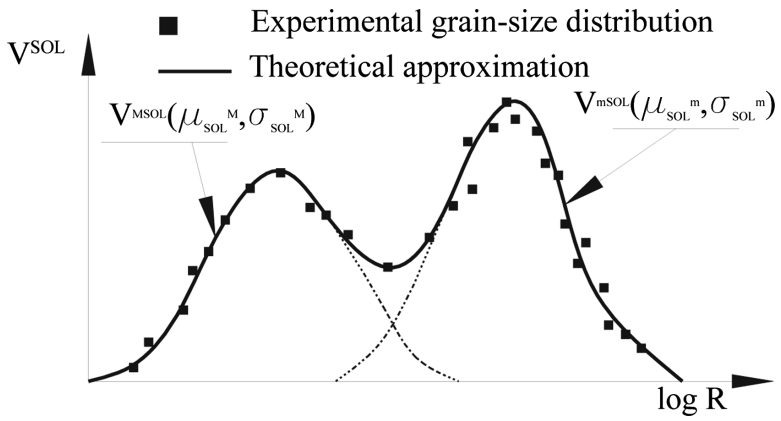

Fig. 2. Fitting theoretical to experimental data of solids volume distribution.

Once fitted, the total volume of solid particles the soil sample appertains, can be computed integrating Eq. (3) from the smallest particle to the largest one:

$$\overline{V^{SOL}} = N\pi \int_0^{\inf} \left(F_{SOL}^{p} f^{MSOL}(R)R^2 + f^{mSOL}(R)R^2\right) dR \tag{7}$$

Obtaining parameters to determine the PSD (Eq. (4)) is not as straightforward. To do this, the fact that there is a unique one to one relationship between a material's PSD and its water retention curve (Dullien 1992; Haines 1927), will be used. This is, parameters for Eq. (4) are those that will serve to fit the experimental Water Retention Curve (WRC).

This process begins constructing a rectangular grid. For this, a set of parameters to evaluate f^{MSOL} and f^{mSOL} are proposed, these will serve to evaluate Eq. (4) which will be a first approach to the PSD.

Once the tentative PSD is evaluated, the number n of sites required to fulfill the needs of the grid can be determined since $f = n/N$. It is important to notice that, randomness is of paramount importance. Therefore, the grid will be constructed taking an element corresponding to each size of the grid randomly and placing it randomly within the grid until very spot of the network is filled by a site. The same happens for the bonds distribution.

During a wetting process, all sites are initially dried, then suction is reduced by steps, and the grid is analyzed to identify those cavities that can be filled with water (see Fig. 3(a)). As stated by Rojas et al. (2011) This is done by identifying those cavities that comply with the following rules that lead pores to saturate: (a) its radius R must be smaller than the critical value R_C given by the Young–Laplace equation, and (b) it must be connected to the bulk of water following a continuous path from the boundaries.

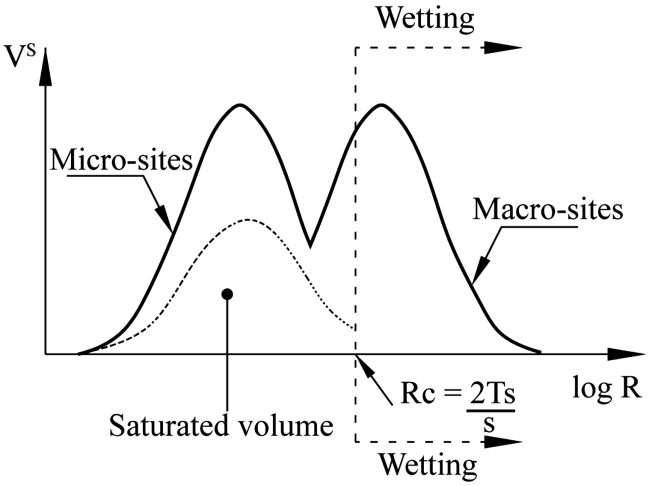

Fig. 3. Wetting-drying processes simulated from a certain PSD.

The Young-Laplace equation writes $s = \mu_a - \mu_w = 2T_S \cos\phi / R_C$ (Lu and Likos 2004), where ϕ is the contact angle which is usually considered as 0 and $T_S = 7.36\,\mathrm{N/m}$ represents the air-water interfacial tensional force. Hence the critical radius can be computed as follows:

$$R_C = \frac{2T_S}{S} \tag{8}$$

For the case of a drying process, a site will dry when it complies with the following conditions: (a) the radius R of the site is larger than the critical radius R_C and (b) it must be connected to the boundaries by a continuous path of dried pores.

With every suction increase/decrease, the rectangular grid is analyzed to search for sites that comply with these two conditions during a drying or wetting path, respectively. It can be seen from Fig. 3 that the total volume supersedes the saturated volume of pores. This is because not all sites are able to saturate or dry according to the previous two established conditions.

The water retention expression is then, that of:

$$Sr(R) = \frac{Vw}{Vv} \tag{9}$$

Where Vw is the volume of water-saturated sites that the grid appertains up to the suction value corresponding to R_C, and Vv is the total volume of the sites of the grid.

3.4 Pore-Size Distribution Evolution

Several reported results on the evolution of the PSD with volumetric strains induced either by increasing suction or by applied mean net stresses indicate that the macropores distribution is the one that seems to be affected the most (Cui et al. 2002; Koliji et al. 2006; Simms and Yanful 2005; Thom et al. 2007). That is, function $f^{MS}\left(\mu^M_{SOL}, \sigma^M_{SOL}\right)$ changes by shifting towards smaller sizes as the soil reduces its void ratio by any means. However, its shape does not seem to change. For this reason, compressive strains will be expressed as a shifting of the f^{MS} changing μ^M_{SOL} solely.

4 Numerical-Experimental Result Comparisons

Perón (2008) evaluate the water retention curve of a Bioley Silt, an inorganic clay of medium plasticity. Samples were fabricated with a water content of 1.5 times their liquid limit, thus ensuring a saturated state. Then, the wet material was poured into a small cylindrical mold of 50 mm diameter and 10 mm height. A goal of this was to study the volume and saturation changes of soils induced by suction The molds containing the wet samples were placed within a pressure plate extractor to measure the water retention curve.

Figure 4 shows the cumulative theoretical GSD which was fitted to the experimental GSD using Eq. (3). Figure 5 shows a theoretical-experimental fitting of the soil-water characteristic curve using the porous model herein.

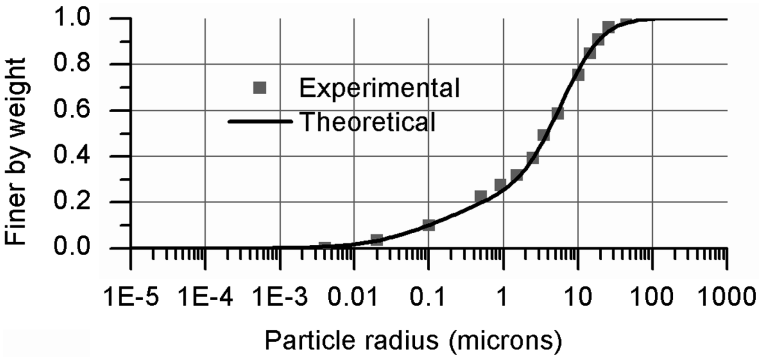

Fig. 4. GSD (Fitted and experimental) $\mu_{SOL}^{M} = -0.2$, $\sigma_{SOL}^{M} = 1.0$, $\mu_{SOL}^{m} = -9.5$, $\sigma_{SOL}^{m} = 2.0$, and $F_{SOL}^{p} = 0.000008$.

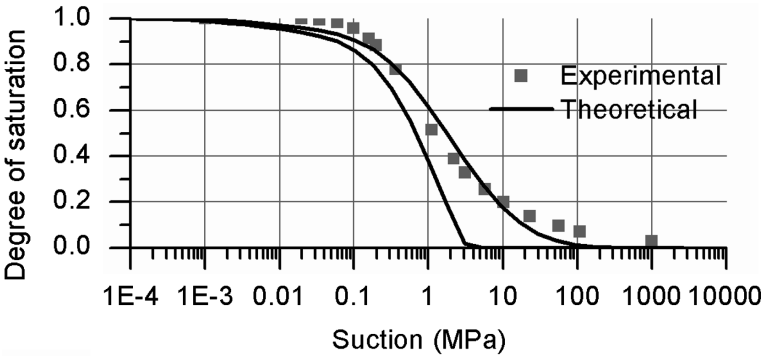

Fig. 5. Differential PSD (fitted and experimental) $\mu_{S}^{M} = -2.5$, $\sigma_{S}^{M} = 1.7$, $\mu_{S}^{m} = -8.05$, $\sigma_{S}^{m} = 1.7$ and $F_{S}^{p} = 0.000001$.

The resulting PSDs and GSDs (predicted) are depicted in Fig. 6. Very important to note from Fig. 6 is that superimposing the macro-solids and macro-sites distributions exhibits a clear resemblance on the range of sizes distribution (peak and distribution). The same for the micro-solids and the micro-sites distributions. This may be an intuitive idea, however, the model confirms this, as stated by Rojas et al. (2011).

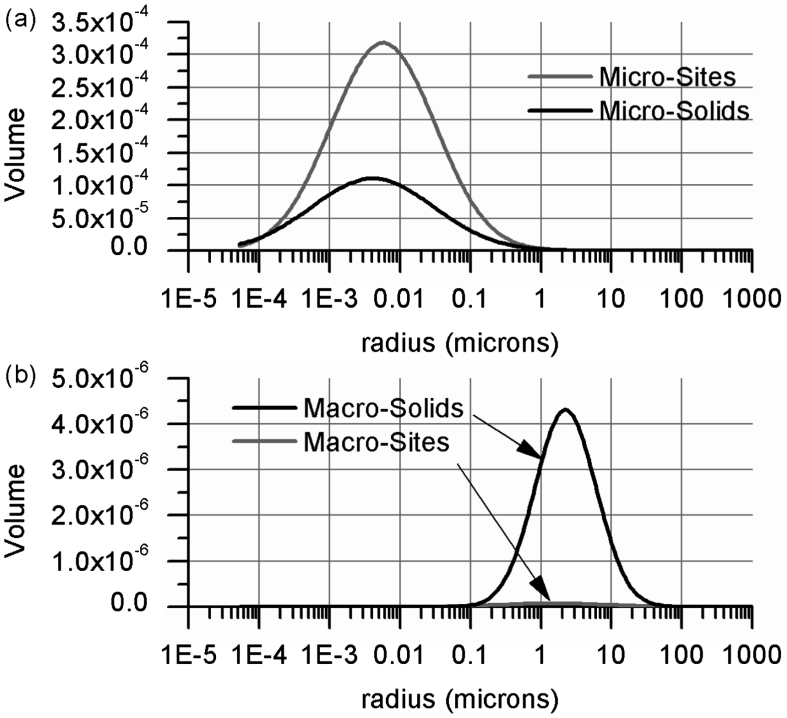

Fig. 6. (a): Predicted micro-solids and micro-sites distributions. (b): Predicted macro-solids and macro-sites distributions.

The relationship between void ratio and suction experimentally evaluated by Perón (2008) is contained in Fig. 7. The initial void ratio of the saturated poured slurry is 0.82 at suction of 19 kPa. The shrinking limit is at a void ratio between 0.60 and 0.58 and a suction value that ranges between 131 and 196 kPa. Using Eq. (6) it is possible to

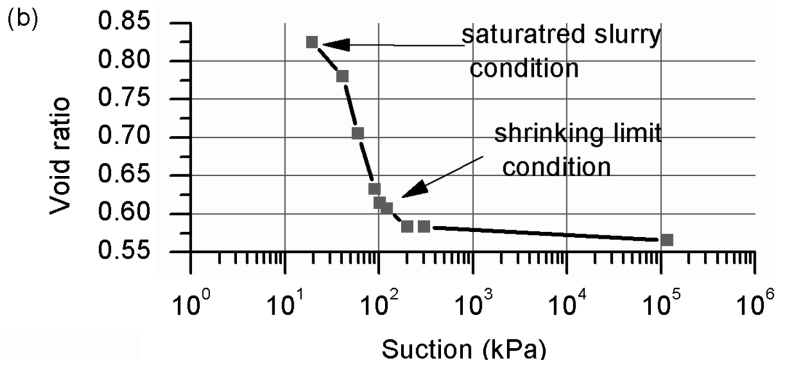

Fig. 7. Experimental relationship between void ratio and suction increments for a Bioley Silt (Perón 2008).

compute the void ratio of the material corresponding to the PSD and GSD of Fig. 6. This retrieves a void ratio of 0.62 which resembles to the real shrinking limit condition.

The model is used to predict the evolution of the PSD. Figure 8 depicts the macropore evolution at the initial saturated slurry and at the shrinking limit condition. This was achieved by increasing the μ_{SOL}^{M} parameter solely as explained earlier.

The macropores depicted on Fig. 8 are used to compute the WRCs at the initial saturated slurry conditions and at the shrinking limit (see Fig. 9).

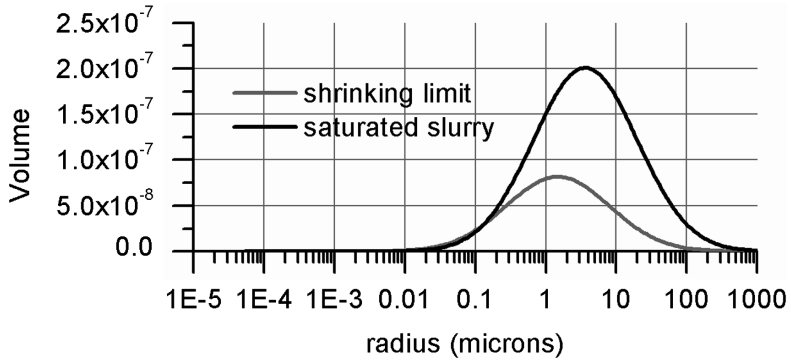

Fig. 8. Predicted evolution of macro-sites to represent the WRC evolution.

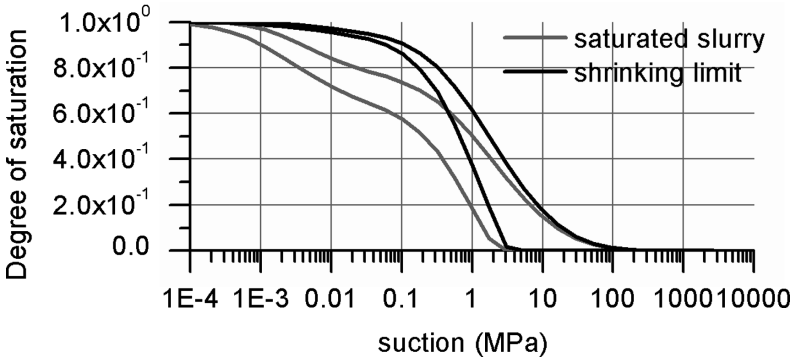

Fig. 9. Predicted WRC at the initial conditions and at the shrinking limit.

Note that, as stated by Perón (2008), the shrinking limit clearly appears at the transition between the saturated and unsaturated condition (i.e. at the suction corresponding to the air entry value).

Here, the shifting of the WRC depicted in Fig. 9, predicted with the presented solid porous model, is in accordance with experimental observations where different WRCs are evaluated for soils with different densities (Ng and Pang 2000; Sun et al. 2007). This shifting occurs due to the compression of the larger pores at early stages of suction

increments which make all the voids remain in a saturated state regardless of the material water content. Further suction increments seem to have a reduced amount of importance on volume strains after the air entry value as it is for the shrinking limit of the material. This is of paramount importance, since this leads to additional tensile stresses that are the reactions to the tendency of the water in tensile state to shrink the material, leading to the to tensile strength as reported by Perón (2008).

5 Conclusions

A mechanism for the evolution of the PSD has been proposed. This enables coupling a constitutive elastoplastic model at high level due to the natural coupling between macroscopic strains and microstructure provided by the solid porous model presented in this paper. This arises from a comprehensive understanding of the behavior and modeling of microstructure considering the PSD as its main expression. Further work needs to be done to understand the evolution of PSD for highly expansive soils.

Acknowledgments. Financial support from the Universidad de Guanajuato in Mexico is greatly acknowledged.

References

Alonso, E.E., Pereira, J.M., Vaunat, J., Olivella, S.: A microstructurally based effective stress for unsaturated soils. Géottechnique **60**(12), 913–925 (2010)

Arroyo, H., Rojas, E.: Fully coupled hydromechanical model for compacted soils. Comptes Rendus Mecanique **347**(1), 1–18 (2019)

Cui, Y.J., Loiseau, C., Delage, P.: Microstructure changes of a confined swelling soil due to suction controlled hydration. In: Jucá, J.F.T., Campos, T., Marinho, F.A.M. (eds.) Unsaturated Soils, pp. 593–598. Balkema, Leiden (2002)

Dullien, F.A.L.: Porous Media: Fluid Transport and Pore Structure. Academic Press, San Diego (1992)

Haines, W.B.: Studies in the physical properties of soils: IV. A further contribution to the theory of capillary phenomena in soil. J. Agric. Sci. **17**(02), 264–290 (1927)

Koliji, A., Laloui, L., Cuisinier, O., Vulliet, L.: Suction induced effects on the fabric of a structured soil. Transp. Porous Med. **64**, 261–278 (2006)

Lu, N., Likos, W.J.: Unsaturated Soil Mechanics. Wiley, New York (2004)

Ng, C.W.W., Pang, Y.W.: Influence of stress state on soil-water characteristics and slope stability. J. Geotech. Geoenviron. Eng. **126**, 157–166 (2000)

Perón, H.: Desiccation Cracking of Soils (Ph.D.), École Polytechnique Fédérale de Lausanne (2008)

Perón, H., Hueckel, T., Laloui, L., Hu, L.: Fundamentals of desiccation cracking of fine-grained soils: experimental characterisation and mechanisms identification. Can. Geotech. J. **46**(10), 1177–1201 (2009)

Rojas, E., Horta, J., López-Lara, T., Hernández, J.B.: A probabilistic solid porous model to determine the shear strength of unsaturated soils. Prob. Eng. Mech. **26**(3), 481–491 (2011)

Roscoe, K.H., Burland, J.B.: On the generalized stress-strain behavior of 'wet' clay. Engineering Plasticity, pp. 535–609. Cambridge University Press, Cambridge (1968)

Simms, P.H., Yanful, E.K.: A pore-network model for hydro-mechanical coupling in unsaturated compacted clayey soils. Can. Geotech. J. **42**(2), 499–514 (2005)

Sun, D.A., Sheng, D.C., Cui, H.B., Sloan, S.W.: A density-dependent elastoplastic hydro-mechanical model for unsaturated compacted soils. Int. J. Numer. Anal. Meth. Geomech. **31** (11), 1257–1279 (2007)

Thom, R., Sivakumar, R., Sivakumar, V., Murray, E.J., Mackinnon, P.: Pore size distribution of unsaturated compacted kaolin: the initial states and final states following saturation. Géotechnique **57**(5), 469–474 (2007)